Phase Separation and Crystallization of Hemoglobin C in Transgenic Mouse and Human Erythrocytes

Joseph E. Canterino,* Oleg Galkin,‡ Peter G. Vekilov,‡§ and Rhoda Elison Hirsch*†
*Department of Medicine and †Department of Anatomy and Structural Biology, Albert Einstein College of Medicine, Bronx, New York; and ‡Department of Chemical and Biomolecular Engineering and §Department of Chemistry, University of Houston, Houston, Texas

ABSTRACT Individuals expressing hemoglobin C (β6 Glu→Lys) present red blood cells (RBC) with intraerythrocytic crystals that form when hemoglobin (Hb) is oxygenated. Our earlier in vitro liquid-liquid (L-L) phase separation studies demonstrated that liganded HbC exhibits a stronger net intermolecular attraction with a longer range than liganded HbS or HbA, and that L-L phase separation preceded and enhanced crystallization. We now present evidence for the role of phase separation in HbC crystallization in the RBC, and the role of the RBC membrane as a nucleation center. RBC obtained from both human homozygous HbC patients and transgenic mice expressing only human HbC were studied by bright-field and differential interference contrast video-enhanced microscopy. RBC were exposed to hypertonic NaCl solution (1.5–3%) to induce crystallization within an appropriate experimental time frame. L-L phase separation occurred inside the RBC, which in turn enhanced the formation of intraerythrocytic crystals. RBC L-L phase separation and crystallization comply with the thermodynamic and kinetics laws established through in vitro studies of phase transformations. This is the first report, to the best of our knowledge, to capture a temporal view of intraerythrocytic HbC phase separation, crystal formation, and dissolution.

INTRODUCTION

Individuals expressing hemoglobin C (β6 Glu → Lys) (HbC) manifest red blood cells (RBC) with intraerythrocytic Hb crystals (1) that form when Hb is in the oxygenated state (2). The formation of these crystals initiates the pathophysiology of homozygous CC disease and contributes to the significantly more severe heterozygous SC disease. (For a review of the clinical manifestations, see Nagel and Steinberg (3)). Selective pressure for the β^C-globin gene exists because of its protective effects against malaria (4). RBC membrane alterations are shown to underlie the protective effects of HbC to malaria (e.g., Tokumasu et al. (5) and Fairhurst et al. (6)).

We have directed our efforts toward understanding the molecular mechanisms involved in the high propensity for liganded HbC to form crystals (7–12). Previous investigations, carried out in vitro in the presence of concentrated phosphate buffer, revealed that HbC crystals grow by the addition of single Hb molecules to special growth sites (kinks) on the crystal surface. These sites are located along the edges of unfinished crystalline layers, which are generated by dislocations or two-dimensional nucleation on the crystal surface (11). The solubility of HbC crystals is very sensitive to temperature and decreases as temperature is raised (8). In vitro, 1), HbC crystals nucleate following classical mechanisms of homogeneous nucleation, whereby local concentration fluctuations result in the crystalline nucleus at a random location and at a random moment (8), and 2), liganded HbC shows a significant propensity for reversible liquid-liquid (L-L) phase separation, whereby the resulting phase diagrams provide evidence that liganded HbC exhibits a stronger net intermolecular attraction with a longer range than liganded HbS and HbA (13).

Bright-field and differential interference contrast (DIC) microscopy showed that although some precrystalline aggregates of HbC form inside the dense Hb protein droplets, most crystals grow from the edge of the droplets or aggregates (13). This observation is not surprising since edge effects on protein crystal growth have been previously reported (14–17). On the other hand, in some systems the crystal readily forms inside the dense phase droplets (18). Dense liquid droplets were also found to serve as preferential locations for the nucleation and growth of polymers of sickle cell Hb, another Hb mutant (β6 Glu→Val) (19). The control parameter that determines whether crystals nucleate inside of dense liquid droplets appears to be dependent on viscosity (20): in highly viscous environments, molecular motion is hampered and the molecules cannot arrange themselves into ordered crystalline nuclei. Yet, it was found that protein solutions increase their concentration as they approach an interface (21), and rapid diffusion of molecules at L-L interfaces accelerates nucleation (22). Thus, we explained the lack of HbC crystal formation inside the dense phase droplets by the high internal viscosity (13). The higher surface concentration and the higher mobility at the droplet surface are the main factors underlying the enhancement of nucleation in the presence of dense liquid droplets. In studies of human homozygous HbC RBC (23), precrystalline aggregates have been observed in higher-viscosity RBC compared to normal

Submitted December 12, 2007, and accepted for publication June 13, 2008.

Address reprint requests to Dr. Rhoda Elison Hirsch, Dept. of Medicine and Dept. of Anatomy and Structural Biology, Albert Einstein College of Medicine (Ullmann 925), Bronx, NY 10461. E-mail: rhirsch@aecom.yu.edu.

Joseph E. Canterino is currently a medical student at The State University of New York Downstate Medical Center, Brooklyn, New York.

Editor: Ron Elber.

© 2008 by the Biophysical Society
0006-3495/08/10/4025/09 $2.00

doi: 10.1529/biophysj.107.127324

HbA RBC, and a temperature-dependent HbC crystallization similar to our in vitro findings (8,9,13,24) has been reported.

In the study presented here, three questions are addressed:

1. Does L-L phase separation occur in HbC red blood cells? This question is related to the broader issue of the cytosolic phase state of various cells. There has been speculation that the free solution in the cytosol may be heterogeneous and contain several liquid phases in dynamic equilibrium (25).
2. Is L-L phase separation related to the formation of crystals inside the RBC cytosol? This question is related to the mechanism of formation of ordered phases in living organisms, some of which have physiological functional significance (26–28).
3. Is crystal formation inside the RBC cytosol subject to thermodynamic and kinetic laws that govern phase transformations according to Gibbs and Volmer (29,30)?

For this investigation, RBC from human CC individuals and transgenic HbC full knockout mouse (HbC full KO, a mouse model that expresses solely human HbC and no mouse globins (31)) were studied. The transgenic mouse HbC full KO RBC is a good model for these studies because it was recently demonstrated that human HbC (and human HbS and HbE) bind to the mouse RBC membrane with greater affinity than mouse globins (32), paralleling the higher affinity of these mutant Hbs to the human RBC membrane (33,34). The transgenic HbC mouse RBC is similar in phenotype to human CC RBC (31) and, moreover, provides unlimited and ready access to CC RBC. Evidence is presented to answer the questions enumerated above and demonstrate a role for the RBC membrane as a nucleation center in intraerythrocytic HbC crystals. This is the first report, to the best of our knowledge, to capture the in situ temporal stages of intraerythrocytic HbC crystal formation and dissolution.

MATERIALS AND METHODS

Human venous blood

Human venous blood was obtained from human donors homozygous for HbC, with informed consent, using a protocol based on the National of Institutes of Health guidelines and approved by the Committee on Clinical Investigations/Institutional Review Board of the Albert Einstein College of Medicine. Blood was collected in heparinized vacutainer tubes. Human RBC, washed three times in isotonic saline (human, 0.9 g% (290 mosm)) were placed on a continuous Larex-Percoll density gradient. The dense fraction containing predominantly crystal-containing cells (35) was harvested. These cells were incubated at temperatures of ~37°C and viewed by light microscopy.

HbC transgenic mouse RBC

Under a protocol approved by the AECOM Institute for Animal Studies, blood was drawn from the tail vein of an anesthetized mouse expressing solely human HbC (31) into heparinized isotonic mouse saline (mouse 1.05g% (330 mosm)). Since the transgenic mice were bred on a C57BL/6 (C57) background, RBC from C57 mice were used as controls. Mouse RBC were separated from plasma and washed three times in their respective isotonic saline. To induce maximal crystal formation within an acceptable experimental time frame, the washed RBC were incubated at 37°C in 3% NaCl (1:1 RBC:3% NaCl) from 2 h to up to 4 h. To ensure RBC separation in the microscope field, the incubated RBC suspension was further diluted (one part incubated RBC : seven parts 3% NaCl), and from this a 3-μL aliquot was placed on a glass slide and viewed by light microscopy and video-enhanced DIC microscopy. Then ~10 μL isotonic saline (mouse) were added to the coverslip edge and crystal dissolution was recorded by video-enhanced DIC microscopy as described in Chen et al. (13).

To assess the sensitivity of crystallization to temperature and composition variations, a chamber was created by gluing a coverslip, a spacer, and two ports to the glass slide. The two ports allowed exchange of the solution in which the RBC were incubated. A brass box with two ports connected to a temperature-controlling water circulator was glued to the slide. Temperature was measured with an HH 506R thermocouple thermometer (Omega Engineering, Stamford, CT) with 0.1°C accuracy and input to a computer using a serial port. The cells were attached to the bottom of the slide using the following procedure: The chamber was filled with poly-L-lysine solution for 20 min and then washed with deionized water. The chamber was then filled with a solution of RBC and kept stationary for 20 min to allow the cells to adhere to the slide. Unattached cells were carefully washed away by passing NaCl solution through the chamber. The initial temperature for the experiments was set to 37°C using a water bath. The setup was mounted on a Leica DM R straight microscope and viewed using DIC optics: a 63× HCX APO L U-V-I water immersion objective, and a 0.90 S1 achromatic condenser (see Weber et al. (49)). Pictures were taken with a Hitachi VCC-151 color video camera, FlashPoint-3D frame grabber (Integral Technologies, Indianapolis, IN).

RESULTS AND DISCUSSION

Liquid-liquid phase separation

To test whether L-L phase separation occurs in the cytosol of RBC, two sources of HbC containing RBC were studied: 1), the RBC dense fraction (separated on a Percoll-Larex gradient) obtained from human CC patients; and 2), RBC from transgenic mice expressing exclusively human HbC (31). Although the transgenic mouse RBC consists of HbC encased in a mouse membrane with differing proportions of cytosolic components, the transgenic HbC RBC phenotype is very similar to that seen in human CC RBC with increased RBC density, increased MCHC, and increased K:Cl cotransport (31). Therefore, Fabry et al. (31) concluded that HbC is responsible for the abnormal RBC phenotype. Hence, the transgenic HbC mouse RBC serves as a good model for studying HbC crystallization and dissolution in RBC.

To accelerate RBC HbC nucleation and crystal growth within an appropriate experimental time frame, cells were incubated using a hypertonic NaCl solution and studied for indications of L-L phase separation. Significant differences were observed between the RBC containing HbC and normal (C57) mice RBC cells exposed to the hypertonic NaCl solution. The majority of the cells with human HbC exhibited regions of different color density by 150 min incubation (Fig. 1 *A*). The number of cells exhibiting dense edge effects increased exponentially over time (Fig. 2). In some cells, regions of intense coloration appeared along the cell edge (Fig. 1 *B*). In other cells, several round-shaped regions of

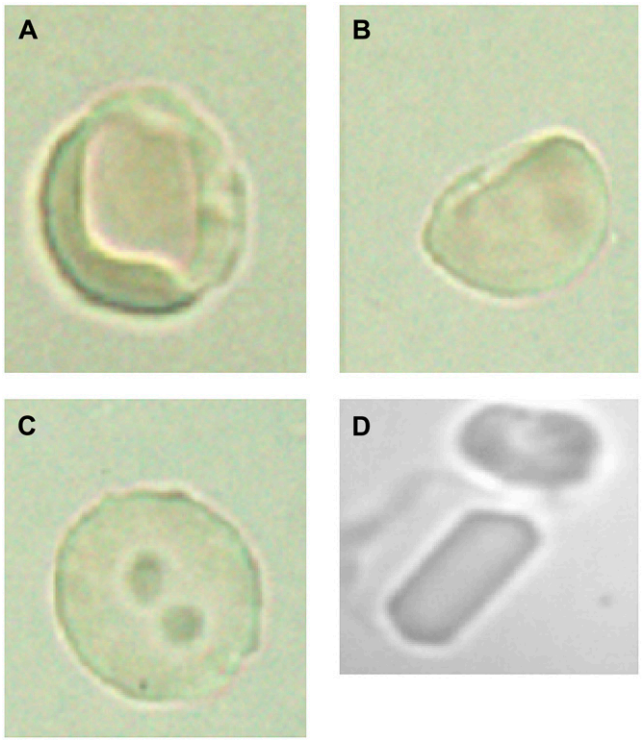

FIGURE 1 Human CC (HbC homozygous) dense RBC exhibiting crystals, heterogeneous Hb densities, and edge effects. Washed human CC RBC were placed and separated according to density on a Percoll-Larex density gradient. The densest fraction was incubated at varying temperatures. At 41°C for 2 h, maximum crystals (*D*) and precrystalline formations appeared (*A–C*).

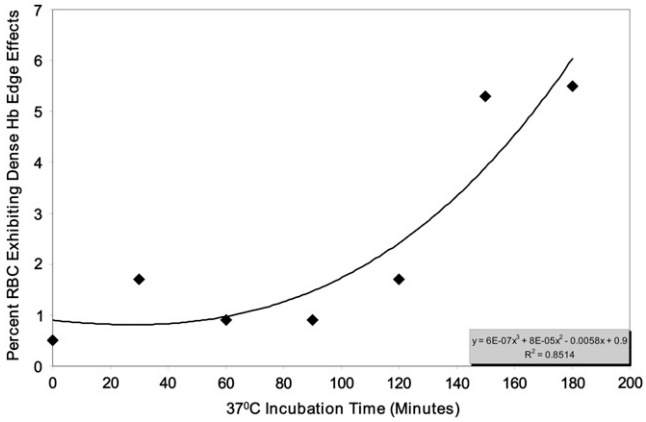

FIGURE 2 Percent RBC from CC transgenic mice expressing solely human HbC that exhibit dense Hb edge effects as a function of incubation time. Packed RBC were incubated using 3% NaCl (1:1 packed RBC:3% NaCl yielded 1.5% NaCl as the starting concentration) at 37°C. Each point represents the average of three separate counts. See Materials and Methods for details.

<1 μm in diameter were randomly scattered throughout the cytosolic intracellular space after more prolonged incubation (4 h) (Fig. 1 *C*). In both cases, the edges between these dense regions and the ''normal'' (less dense) cytosol were sharp. We attribute the high color intensity to higher concentrations of Hb in the dark regions. The sharp edges suggest the presence of a phase boundary, and the round shape suggests that the Hb rich phase is liquid (i.e., that L-L phase separation has occurred). If this phase forms in the vicinity of the cell membrane, it apparently wets it, and this yields the pattern seen in Fig. 1 *B*. If the Hb-rich phase forms away from the cell membrane, it forms drops of solution whose round shape, as shown in Fig. 1 *C*, is determined by the minimization of the surface free energy. It is established that L-L phase separation usually appears as liquid protein droplets characterized by a high protein density. (Details of the principles of L-L phase separation with regard to Hb solutions are discussed at length in Chen et al. (13)).

L-L phase separation is known to be sensitive to solution composition (13). One of the factors known to enhance L-L separation is higher concentrations of electrolytes (36). To further confirm L-L phase separation in the RBC cytosol, cells were exposed to a lower (2.2%) concentration of NaCl. It was observed that the regions of higher Hb concentration, both along the cell edges, as in Fig. 1 *B*, and away from them, as in Fig. 1 *C*, disappear. Reversibility is characteristic of L-L phase separation. Hence, these observations strongly suggest that the formation of Hb-rich borders along the cell membrane and of the Hb-rich droplets inside the RBC is L-L phase separation in the RBC cytosol.

In contrast to the transgenic mice HbC RBC, the fraction of RBC from normal C57Bl control mice exhibiting inhomogeneous Hb concentration is significantly lower and reaches $\sim$5% only after 3 h of incubation. This trend is explained by the higher propensity of HbC in vitro to form a dense liquid phase compared to other Hb variants (13). The mechanistic basis for the specificity of HbC toward this phase transition, as well as its high propensity to nucleate and form crystals, is due to a stronger net intermolecular attraction with a longer range than other Hb variants (13).

Crystal formation

After L-L coexistence was observed in some HbC RBC from the transgenic HbC mouse, further incubation (for $\sim$1 h) led to the formation of intraerythrocytic crystals. Remarkably, crystals formed predominantly in cells displaying L-L phase separation. Examples of the observed crystals are seen in Figs. 1 *D*, 3, and 5–7. All intraerythrocytic crystals were faceted and some were positioned in such a way that the tetragonal dipyramid shape that is typical of HbC crystals (as observed when grown in vitro in concentrated phosphate, and in vivo (2,10,37)) was detectable despite the imaging interference of the cell membrane.

To probe the dissolution behavior of the intraerythrocytic crystals observed in this study, we used two approaches: 1), dilution of the solution around the RBC by the addition of isotonic mouse saline to the coverslip edge; and 2), lowering

temperature. The intraerythrocytic crystals dissolved in minutes after addition of isotonic saline. Crystal dissolution started away from the crystal face closest to the RBC edge. Of note, the smallest remaining part of the melting crystal remained tethered to the RBC edge (presumably the membrane) until loss of the characteristic sharp edges and final dissolution of the crystal occurred (Fig. 3 and the Supplementary Information, Movie S1 and Movie S2, Data S1). In many cases, at a certain point, a dense liquid droplet emerged from the dissolving crystal. This structure was not tethered to the membrane and exhibited Brownian-like motion until final dissolution (see Movie S1 and Movie S2, Data S1).

Observations of Brownian motion of these rounded forms and its fast dissolution are consistent with the properties of dense liquid droplets and L-L phase separation. Therefore, we conclude that L-L phase separation precedes HbC crystallization in the RBC. Furthermore, this emerged dense liquid droplet could have served as the site of nucleation and growth for that crystal.

The dissolution time of the crystals correlates with crystal size, with larger crystals taking longer to dissolve (Fig. 4). A polynomial analysis of the dissolution time with crystal size (area) is used because we are monitoring the cross-sectional area of the crystal in the image plane, and this area should decrease as the product of the rate of retraction on each side. Thus, with a constant dissolution rate, the rate of retraction of each side is linearly dependent on time, and the area decreases as a quadratic dependence. The only assumption made is that the dissolution has reached a steady state, i.e., the number of molecules departing from a unit surface area of the crystal does not change in time. It should be noted that the argument is purely geometrical and contains no assumptions as to whether the kinetics of dissolution at the crystal's surface or diffusion of Hb away from the crystal is the rate-determining step.

A polynomial fit of the time t dependence of the area covered by crystals during dissolution reveals a t^3 law in all 10 tested cases in Fig. 4. If the rate of dissolution of the crystal faces is constant, the area should decrease as t^2. The cubic dependence indicates that the rate of dissolution increases as the crystal size decreases. Such dependencies have been interpreted as evidence for strain in small crystals (38). The likely source of this strain is the unstructured aggregate revealed at the end of dissolution. The generality of the strain suggests that all observed crystals contain such aggregates, and it is likely that the aggregates are the objects upon which heterogeneous nucleation of crystallization occurs.

To test whether intraerythrocytic crystal formation is subject to the laws of thermodynamics that govern all phase transitions, the sensitivity of crystal formation to temperature was examined. Crystals were formed by incubating HbC transgenic mouse RBC in a hypertonic NaCl solution at 37°C (Fig. 5). After crystal formation was detected, using the inlet and outlet ports of the setup described above, this solution was completely replaced by 2.2% NaCl. In this solution, the crystals were stable at 37°C. However, as soon as the temperature was lowered to 35°C, the crystals completely dissolved within ~2 min (Fig. 5). This observation shows that HbC crystallization in RBC follows the same retrograde dependence of solubility on temperature (higher solubility at lower temperature), as seen in vitro (8,24). Regarding the reproducibility and significance of the temperature values, we have observed hundreds of cells under slightly varying conditions. The response to temperature of dissolution and the formation of dense liquid droplets was consistent with all cells observed. The data shown are representative for all observations. Of course, depending upon the exact concentration of the NaCl used in the incubating solution, crystallization equilibrium was reached at expected corresponding different temperatures. Likewise, minor variations in the NaCl concentration led to anticipated slight changes in the exact temperatures of the monitored events. The crystallization of HbC in RBC occurs in a complex cellular environment where fractional environmental differences will have an

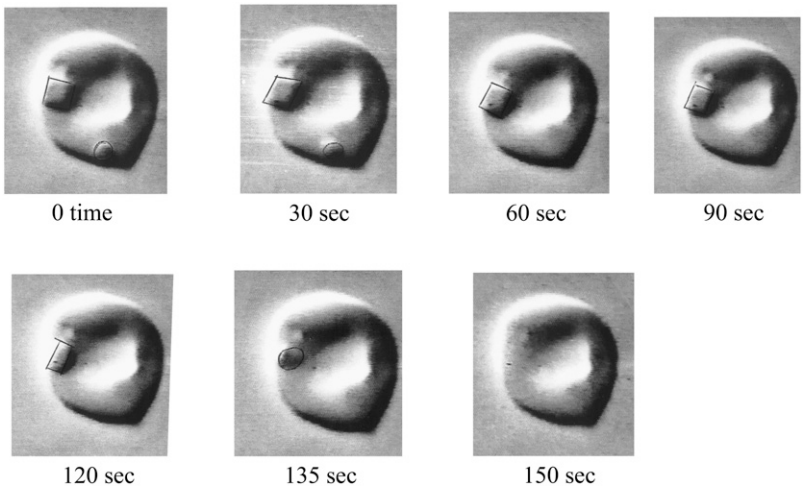

FIGURE 3 Intraerythrocytic HbC crystal dissolution induced by a change in tonicity over time. Video-enhanced DIC microscopy images are stills from a video recording (Movie S1 and Movie S2, Data S1) following crystal dissolution over time (0.1 s in video time corresponds to 5 s in real time). Crystal formation in transgenic mouse RBC containing solely human HbC was induced by incubation with 3%NaCl (1:1 packed RBC:3% NaCl) for 3 h. Crystal dissolution was induced by osmotic change with the addition of ~10 μL isotonic mouse saline to the coverslip edge. In the sequence shown, crystal dissolution occurred within 150 s. See Materials and Methods for complete details of crystal formation and dissolution.

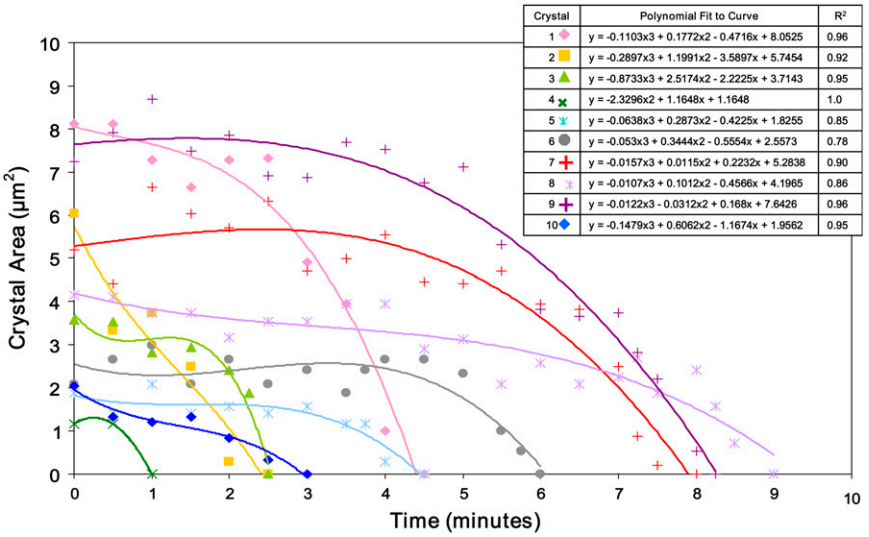

FIGURE 4 Intraerythrocytic HbC crystal dissolution as a function of time. The area of the intraerythrocytic crystal (and during dissolution) was measured from photos taken over time. Crystals 1 and 2, 3 and 4, 5 and 6, and 7–10, respectively, belonged to the same cells (total cells with respect to these crystals: four). All photos were taken at the same magnification. See Fig. 3 caption for methodology.

impact on crystal growth. This is well known for in vitro crystallization, and thus serves as another example of how the observed intraerythrocytic crystal growth exhibits properties of in vitro crystal growth.

To test the reversibility of crystal formation, the crystals shown in the first (left) panel in Fig. 6 were exposed to 2.5% NaCl solution. As shown in Fig. 5, the crystals were stable at 37°C. The temperature was then gradually lowered to 35°C. Surprisingly, the RBC on the right in the left panel formed a crystal only after the initial temperature decrease, at ~36.5°C. This observation means that the cytosol without crystals was supersaturated at this temperature, and was even more supersaturated at the initial 37°C. The lack of crystals in that cell at 37°C indicates that nucleation of the crystal in the RBC cytosol is a process that has to overcome a barrier. In this respect, this crystal formation is analogous to all nucleation processes in vitro (39–41). The likely scenario of crystal nucleation at ~36.5°C is that the initial temperature decrease caused a temperature gradient that induced solution flow in the RBC cytosol (42,43). Solution flow, in turn, enhanced crystal nucleation (44,45) and led to the formation of the crystal seen in the RBC in the right column of Fig. 6.

As the temperature approached and then remained at 35°C, the crystals in both cells partially dissolved. The HbC released upon dissolution of the outer crystal layers increased the HbC concentration in the RBC cytosol to the solubility level and dissolution stopped. This observation shows that the solubility at 35°C in 2.5% NaCl is lower than in a 2.2% NaCl solution. Lower solubility at higher electrolyte concentration is consistent with earlier in vitro observations (8). Furthermore, after the temperature in this experiment was raised to 37°C, the crystal grew back. Thus, crystal growth in the RBC is an entirely reversible process and subject to all thermodynamic controls that govern phase transformations of all substances in vitro. The possibility that the dense red regions or crystals may be Hb amorphous aggregates is ruled out by this reversibility, the round shape of the dense regions, and their fast dissolution (Figs. 6 and 7).

To probe the temperature at which the RBC cytosol is in equilibrium with the crystal, we studied intraerythrocytic crystals that formed after incubation in 3% NaCl at 37°C. The incubating solution was then completely replaced with a 2.5% NaCl final concentration (see Materials and Methods section). The temperature was lowered in steps, waiting for the cessation of dissolution and the establishment of equilibrium between the crystal and cytosol at each temperature step. Fig. 7 shows the steps between 35.7°C and 30.6°C. The single crystal seen in the RBC dissolved completely at 31.0°C (Fig. 7, *right column*), whereas the last small crystals in the RBC (seen in the left column of Fig. 7) dissolved only at 30.6°C. The difference in the two equilibrium

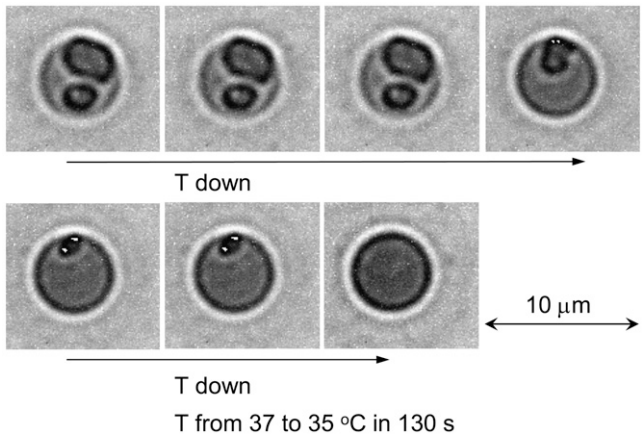

FIGURE 5 Intraerythrocytic HbC crystal dissolution induced by a change in temperature. Imaging by temperature-controlled DIC microscopy demonstrated intraerythrocytic crystals formed upon incubation of RBC at $T =$ 37°C in hypertonic NaCl solution. The incubating solution was replaced by a 2.2% solution. Crystal dissolution started only after T was lowered to 35°C. The accuracy of temperature control is 0.1°C (see Materials and Methods). The crystals were completely dissolved within ~2 min.

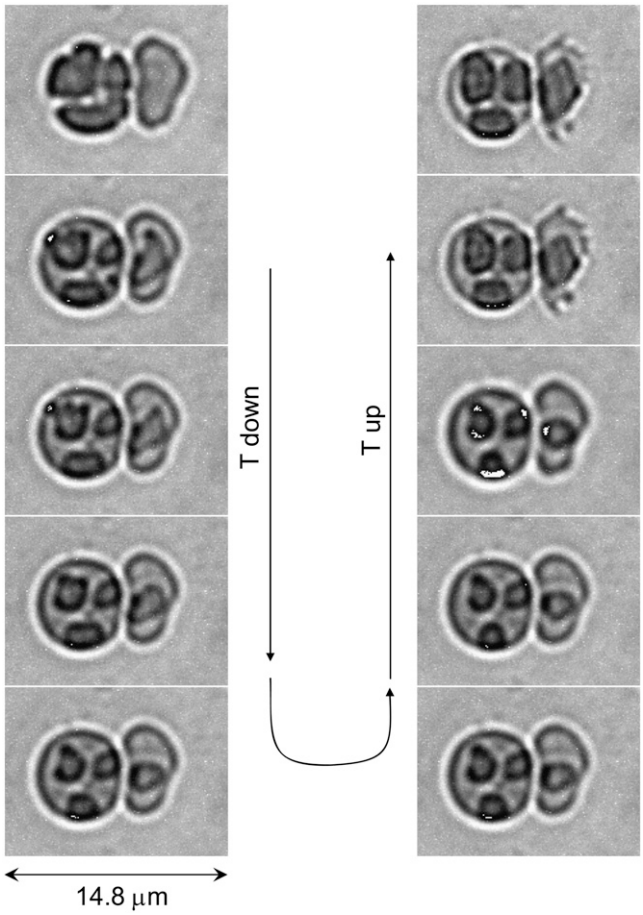

FIGURE 6 Reversibility of intraerythrocytic HbC crystal growth and dissolution. Imaging by temperature-controlled DIC microscopy. Crystals were formed by incubation of RBC at $T = 37$°C in hypertonic NaCl solution. The incubating solution was completely replaced by a 2.5% NaCl solution. Temperature was slowly (over ~1 h) lowered to 35°C. The respective images of the cells are in the left column. The temperature was then raised to the same 37°C. The sequence of images in the right column is from bottom to top. The accuracy of temperature control is 0.1°C (see Materials and Methods).

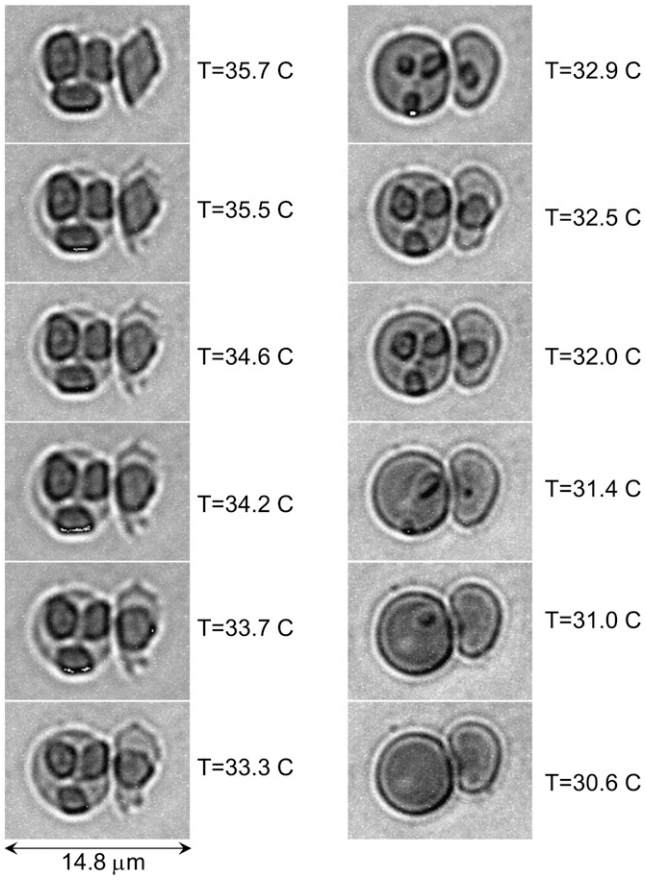

FIGURE 7 Equilibrium between intraerythrocytic HbC crystals and the RBC cytosol. Imaging by temperature-controlled DIC microscopy. Crystals were formed by incubation of RBC at 37°C in 3% NaCl solution. The incubating solution was completely replaced by 2.5% NaCl solution (final concentration). Temperature was lowered in steps from 37°C to 30.6°C; select frames are shown. The accuracy of temperature control is 0.1°C (see Materials and Methods). Temperature was lowered to each subsequent step after equilibrium between crystals and cytosol, as judged from the cessation of dissolution obtained at the previous step. Crystals in different cells dissolved completely at different temperatures, indicating different HbC concentrations in the cells.

temperatures is likely due to different HbC concentrations in the two cells.

Control experiments in which RBC from a control mouse (C57, expressing exclusively mouse Hb single) were incubated in 3% NaCl revealed no crystals. However, after 4 h, a small number of these cells exhibit noncrystalline aggregate forms that are not tethered to the membrane (not shown). If the cells are exposed to isotonic saline, these aggregates shrink in size and move about randomly until they are completely dissolved. Large aggregates, about the diameter of the mouse RBC (~6 μ), are seen in some of the cells and appear striated, suggestive of fibrillar structure.

In summary, induced intraerythrocytic HbC L-L phase separation and crystallization follow many of the thermodynamics and kinetic characteristics of crystal growth processes observed in vitro. However, the presence of the RBC membrane induces specificity of the intracellular crystallization: the tethering of the crystal to the membrane likely indicates a role of the membrane as a preferred center for crystal nucleation, either directly or via the formation of an amorphous aggregate. The phase behavior of HbC in the RBC cytosol differs from the controls not only in its propensity to crystallize, but also in its ability to form dense liquid phases. It should also be noted that, for in vitro solutions of Hb (HbC and HbS), trace amounts of PEG appear to be required for L-L phase separation (e.g., Chen et al. (13) and Galkin et al. (19)). In this study of HbC RBC, no additives were employed other than the hypertonic solutions of NaCl. The findings presented here, suggesting L-L phase separation in the HbC RBC, support our earlier proposal that the RBC may contain components that behave like PEG in vitro to effect L-L phase separation (13). The identification of

these specific components will be the subject of a separate investigation.

Overview of L-L phase separation and the RBC membrane

Nucleation upon the erythrocyte membrane in the formation of the liganded HbC crystal or deoxy HbS polymer now becomes a possibility, especially in consideration of the well-known specific interaction of Hb with the cytosolic side of the RBC membrane. In vitro studies demonstrate that human Hb binds to cytosolic Band 3 (cB3H) of the erythrocyte membrane with an affinity dependent on the Hb variant (HbC>HbA_2>HbS>HbA) (33,34). We recently showed that, in the oxygenated state, HbC and HbS are bound with higher affinity to the transgenic mouse RBC membrane (32).

Crystallographic evidence shows that the cB3H 11 amino acid N-terminus peptide binds to deoxy Hb central cavity residues, including those that bind 2,3 diphosphoglycerate (DPG) (46). However, it has also been established that oxy Hb binds to the cytosolic portion of Band 3, albeit with a lower affinity that deoxy Hb. Whether oxy Hb dimers (in contrast to tetrameric Hb) bind to Band 3 in the RBC remains to be resolved. (See Salhany (47) for a recent overview of oxy and deoxy Hb binding to Band 3.) A recent report by Low and colleagues (48) points to the N-terminus residues 12–23 as a high-affinity site for deoxy Hb, and thus introduces the likelihood that the Hb-Band 3 narrative may be rewritten or certainly further qualified. The complete function of Hb binding to Band 3 (the transmembrane anion exchanger) remains unknown, but evidence strongly suggests that Hb binding to the cytosolic portion of Band 3 may play a significant role in regulating erythrocyte glycolysis, as well as oxygen regulation of RBC properties (48–50). Band 3 is now considered to function within a complex or metabolon, and its interaction with Hb is now implicated in nitric oxide/nitrite transport and physiology (48,51,52).

The high-affinity binding of HbC and HbS to the human RBC membrane with Band 3 implicated (33,34,53) and to the mouse RBC (32) provides a basis for the hypothesis that the membrane may serve as an intraerythrocytic site of nucleation for the deoxygenated HbS polymer (54), and, as suggested in this study, in the formation of the liganded HbC crystal. The possibility that the complex RBC membrane (as well as some RBC cytosolic components) plays a role in HbC nucleation and crystallization was indicated earlier by in vitro studies demonstrating that oxy HbC crystallization is accelerated by the presence of the cytosolic N-terminus domain of human Band 3 and the 11 amino acid N-terminus Band 3 peptide (55). Oxy Hb binding to Band 3 may be explained by the following: oxy/liganded β6 mutant Hbs exhibit an altered central cavity that may give rise to their unique Hb intra- and intermolecular interactions (55–59). Nevertheless, with the data presented in this study, we cannot make any inference regarding the purported site of binding.

In vitro studies of membrane effects on the nucleation of deoxy HbS (recently summarized and readdressed by Aprelev et al. (54)) showed an 80% enhancement of the nucleation rate where deoxy HbS was immediately adjacent to sickle cell membrane open ghosts. These observations for HbS lend support to the study presented here, which shows a propensity of the RBC membrane surface to exhibit both noncrystalline forms and higher ordered forms of HbC. Indeed, the dissolution of the intraerythrocytic crystal that remains bound to the cell surface until it converts to a noncrystalline form is suggestive of a membrane nucleation site for the intraerythrocytic HbC crystal involving initiation or wetting by a dense liquid droplet. The suggested membrane nucleation site is indeed a complex issue, especially in light of new evidence that Hb has a greater affinity for residues 12–23 of the Band 3 N-terminus (48). In vitro studies of mutants HbC and HbS in the presence of this peptide will aid in illuminating the possibility of Band 3 as a nucleation site for oxy/ligandedHbC crystallization or deoxy HbS polymerization.

HbC nucleation on microscopic aggregates of hemichromes bound to the RBC membrane is an alternative possibility that cannot be completely ruled out, since RBC containing HbC exhibit hemichrome aggregates bound to the membrane (34) and enhanced membrane fragility (23). The notion that some HbC ''precrystalline'' structures and the RBC membrane play a secondary role in generating RBC rigidity, fragmentation, and microcytosis, as observed in HbC hemoglobinopathy, has already been suggested in systematic studies of human HbC RBC by Charache et al. (23). (A recent overview of HbC in the RBC can be found in Brittain et al. (60).) The results presented here add to the role of the RBC membrane in this hemoglobinopathy (e.g., alterations in potassium transport observed in both human and mouse HbC RBC (61,62)), and suggest that the HbC RBC membrane or its membrane abnormalities may serve as a nucleation site for HbC crystallization. It is noteworthy that the solubility properties and behavior of HbC within the RBC may seem to be in contrast to in vitro behavior observed with hemolysates (23), but are accounted for by ''unique conditions of the RBC that have yet to be determined'' (63). Elucidation of these unique conditions is under way with the normal and pathologic human RBC and normal C57/Bl mouse RBC proteomes recently described (e.g., 64,65).

The involvement of the cell membrane in the nucleation of higher-ordered proteins is a phenomenon reported in other biosystems, such as in the aggregation of α-synuclein (66). Furthermore, as some of us noted earlier (67), the implication of intracellular L-L phase separation before higher-order aggregation sets the stage for designing drug therapies for various diseases correlated with protein aggregates, polymers, or crystals.

SUPPLEMENTARY MATERIAL

To view all of the supplemental files associated with this article, visit www.biophysj.org.

We thank Dr. Mary E. Fabry and her associate, Sandra E. Suzuka, for allowing us to draw minimal blood from the HbC full KO transgenic mice according to approved protocols of the Animal Institute of the Albert Einstein College of Medicine. Venous blood was obtained from CC patients using an Albert Einstein College of Medicine CCI/IRB-approved protocol. We acknowledge Dr. Qiuying Chen for her efforts with early preliminary studies, and Michael Cammer of the Albert Einstein College of Medicine Analytical Imaging Center for excellent technical support with the technical conversion of the videos (Movie S1 and Movie S2 in the Supplementary Material, Data S1).

This work was partially supported by the American Heart Association Heritage Affiliate (0256390T and 0755906T), National Institutes of Health (R21 DK-064123 and NIH HL-091474), and National Science Foundation (G092524).

REFERENCES

1. Diggs, L. W., A. P. Kraus, D. B. Morrison, and R. P. Rudnicki. 1954. Intraerythrocytic crystals in a white patient with hemoglobin C in the absence of other types of hemoglobin. *Blood.* 9:1172–1184.
2. Hirsch, R. E., C. Raventos-Suarez, J. A. Olson, and R. L. Nagel. 1985. Ligand state of intraerythrocytic circulating HbC crystals in homozygote CC patients. *Blood.* 66:775–777.
3. Nagel, R. L., and M. H. Steinberg. 2001. Hemoglobin SC Disease and HbC Disorders. *In* Disorders of Hemoglobin: Genetics, Pathophysiology, and Clinical Management. M. H. Steinberg, B. G. Forget, D. R. Higgs, and R. L. Nagel, editors. Cambridge University Press, Cambridge, UK. 711–785.
4. Modiano, D., G. Luoni, B. S. Sirima, J. Simpore, F. Verra, A. Konate, E. Rastrelli, A. Olivieri, C. Calissano, G. M. Paganotti, L. D'Urbano, I. Sanou, A. Sawadogo, G. Modiano, and M. Coluzzi. 2001. Haemoglobin C protects against clinical *Plasmodium falciparum* malaria. *Nature.* 414:305–308.
5. Tokumasu, F., R. M. Fairhurst, G. R. Ostera, N. J. Brittain, J. Hwang, T. E. Wellems, and J. A. Dvorak. 2005. Band 3 modifications in *Plasmodium falciparum*-infected AA and CC erythrocytes assayed by autocorrelation analysis using quantum dots. *J. Cell Sci.* 118:1091–1098.
6. Fairhurst, R. M., D. I. Baruch, N. J. Brittain, G. R. Ostera, J. S. Wallach, H. L. Hoang, K. Hayton, A. Guindo, M. O. Makobongo, O. M. Schwartz, A. Tounkara, O. K. Doumbo, D. A. Diallo, H. Fujioka, M. Ho, and T. E. Wellems. 2005. Abnormal display of PfEMP-1 on erythrocytes carrying haemoglobin C may protect against malaria. *Nature.* 35:1117–1121.
7. Hirsch, R. E., R. E. Samuel, N. A. Fataliev, M. J. Pollack, O. Galkin, P. G. Vekilov, and R. L. Nagel. 2001. Differential pathways in oxy and deoxy HbC aggregation/crystallization. *Proteins Struct. Funct. Genet.* 42:99–107.
8. Vekilov, P. G., A. R. Feeling-Taylor, D. N. Petsev, R. L. Nagel, and R. E. Hirsch. 2002. Intermolecular interactions, nucleation, and thermodynamics of crystallization of hemoglobin C. *Biophys. J.* 83:1147–1156.
9. Vekilov, P. G., A. Feeling-Taylor, and R. E. Hirsch. 2003. Nucleation and crystal growth of hemoglobins: the case of HbC. *In* Methods in Hemoglobin Disorders (Series in Molecular Medicine). R. L. Nagel, editor. Humana Press, Totowa, NJ. 155–193.
10. Dewan, J. C., A. Feeling-Taylor, Y. A. Puius, L. Patskovska, Y. Patskovsky, R. L. Nagel, S. C. Almo, and R. E. Hirsch. 2002. Structure of mutant human carbonmonoxyhemoglobin C (βE6K) at 2.0Å resolution. *Acta Crystallogr. D Biol. Crystallogr.* 58:2038–2042.
11. Ferrone, F. A., J. Hofrichter, and W. A. Eaton. 1985. Kinetics of sickle hemoglobin polymerization. II. A double nucleation mechanism. *J. Mol. Biol.* 183:611–631.
12. Patskovska, L. N., Y. V. Patskovsky, S. C. Almo, and R. E. Hirsch. 2005. COHbC and COHbS crystallize in the R2 quaternary state at neutral pH in the presence of PEG 4000. *Acta Crystallogr.* D61:566–573.
13. Chen, Q. Y., P. G. Vekilov, R. L. Nagel, and R. E. Hirsch. 2004. Liquid-liquid phase separation in hemoglobins: distinct aggregation mechanisms of the β6 mutants. *Biophys. J.* 86:1702–1712.
14. McPherson, A. 1985. Crystallization of proteins by variation of pH or temperature. *Methods Enzymol.* 114:120–125.
15. Ray Jr., W. J., and J. M. Puvathingal. 1986. The effect of polyethylene glycol on the growth and dissolution rates of a crystalline protein at high salt concentration. phosphoglucomutase. *J. Biol. Chem.* 261:11544–11549.
16. Kuznetsov, Y. G., A. J. Malkin, and A. McPherson. 1999. AFM studies of the nucleation and growth mechanisms of macromolecular crystals. *J. Cryst. Growth.* 196:489–502.
17. Kuznetsov, Y. G., A. J. Malkin, R. W. Lucas, M. Plomp, and A. McPherson. 2001. Imaging of viruses by atomic force microscopy. *J. Gen. Virol.* 82:2025–2034.
18. Vivares, D., E. W. Kaler, and A. M. Lenhoff. 2005. Quantitative imaging by confocal scanning fluorescence microscopy of protein crystallization via liquid-liquid phase separation. *Acta Crystallogr. D Biol. Crystallogr.* 61:819–825.
19. Galkin, O., K. Chen, R. L. Nagel, R. E. Hirsch, and P. G. Vekilov. 2002. Liquid-liquid separation in solutions of normal and sickle cell hemoglobin. *Proc. Natl. Acad. Sci. USA.* 99:8479–8483.
20. Pan, W., A. B. Kolomeisky, and P. G. Vekilov. 2005. Nucleation of ordered solid phases of proteins via a disordered high-density state: phenomenological approach. *J. Chem. Phys.* 122:174905.
21. MacRitchie, P., and A. E. Alexander. 1963. Kinetics of adsorption of proteins at interfaces. Part II. The role of pressure barriers in adsorption. *J. Colloid Sci.* 18:464–469.
22. Lin, H., S.-T. Yau, and P. G. Vekilov. 2003. Dissipating step bunches during crystallization under transport control. *Phys. Rev. E Stat. Nonlin. Soft Matter Phys.* 67:0031606.
23. Charache, S., C. L. Conley, D. F. Waugh, R. J. Ugoretz, and J. R. Spurrell. 1967. Pathogenesis of hemolytic anemia in homozygous hemoglobin C disease. *J. Clin. Invest.* 46:1795–1811.
24. Feeling-Taylor, A. R., R. M. Banish, R. E. Hirsch, and P. G. Vekilov. 1999. Miniaturized scintillation technique for protein solubility determinations. *Rev. Sci. Instrum.* 70:2845–2849.
25. Brooks, D. E. 2000. Can cytoplasm exist without undergoing phase separation? *Int. Rev. Cytol.* 192:321–330.
26. Dodson, G., and D. Steiner. 1998. The role of assembly in insulin's biosynthesis. *Curr. Opin. Struct. Biol.* 8:189–194.
27. Dobson, C. M. 2002. Getting out of shape. *Nature.* 418:729–730.
28. Doye, J. P. K., and W. C. K. Poon. 2006. Protein crystallization in vivo. *Curr. Opin. Colloid Interface Sci.* 11:40–46.
29. Chaikin, P. M., and T. C. Lubensky. 1995. Principles of Condensed Matter Physics. Cambridge University Press, Cambridge, UK.
30. Vekilov, P. G., and A. A. Chernov. 2002. The physics of protein crystallization. *In* Solid State Physics. H. Ehrenreich and F. Spaepen, editors. Academic Press, New York. 1–147.
31. Fabry, M. E., J. R. Romero, S. M. Suzuka, J. G. Gilman, A. Feeling-Taylor, E. Odunusi, S. M. Factor, E. E. Bouhassira, C. Lawrence, and R. L. Nagel. 2000. Hemoglobin C in transgenic mice: effect of HbC expression from founders to full mouse globin knockouts. *Blood Cells Mol. Dis.* 26:331–347.
32. Chen, Q., T. C. Balazs, R. L. Nagel, and R. E. Hirsch. 2006. Human and mouse hemoglobin association with the transgenic mouse erythrocyte membrane. *FEBS Lett.* 580:4485–4490.
33. Shaklai, N., J. Yguerabide, and H. M. Ranney. 1977. Interaction of hemoglobin with red blood cell membranes as shown by a fluorescent chromophore. *Biochemistry.* 16:5585–5592.

34. Reiss, G. H., H. M. Ranney, and N. Shaklai. 1982. Association of hemoglobin C with erythrocyte ghosts. *J. Clin. Invest.* 170:946–952.

35. Fabry, M. E., D. K. Kaul, C. Raventos, S. Baez, R. Rieder, and R. L. Nagel. 1981. Some aspects of the pathophysiology of homozygous Hb CC erythrocytes. *J. Clin. Invest.* 67:1284–1291.

36. Muschol, M., and F. Rosenberger. 1997. Liquid-liquid phase separation in supersaturated lysozyme solutions and associated precipitate formation/crystallization. *J. Chem. Phys.* 107:1953–1962.

37. Hirsch, R. E., M. J. Lin, and R. L. Nagel. 1988. The inhibition of hemoglobin C crystallization by hemoglobin F. *J. Biol. Chem.* 263:5936–5939.

38. Vekilov, P. G., Y. G. Kuznetsov, and A. A. Chernov. 1990. Dissolution morphology and kinetics of (101) ADP face; mild etching of surface defects. *J. Cryst. Growth.* 102:706–716.

39. Gibbs, J. W. 1876. On the equilibrium of heterogeneous substances. *Trans. Connect. Acad. Sci.* 3:108–248.

40. Gibbs, J. W. 1878. On the equilibrium of heterogeneous substances. *Trans. Connect. Acad. Sci.* 16:343–524.

41. Kashchiev, D. 2000. Nucleation. Basic Theory with Applications. Butterworth-Heinemann, Oxford, UK.

42. Bird, R. B., W. E. Stewart, and E. N. Lightfoot. 1960. Transport Phenomena. John Wiley and Sons, New York.

43. Shiga, T., N. Maeda, and K. Kon. 1990. Erythrocyte rheology. *Crit. Rev. Oncol. Hematol.* 10:9–48.

44. Penkova, A., W. Pan, F. V. Hodjaoglu, and P. G. Vekilov. 2006. Nucleation of protein crystals under the influence of solution shear flow. *Ann. N. Y. Acad. Sci.* 1077:214–231.

45. Blaak, R., S. Auer, D. Frenkel, and H. Löwen. 2004. Homogenous nucleation of colloidal melts under the influence of shearing fields. *J. Phys. Condens. Matter.* 16:S3873–S3884.

46. Walder, J. A., R. Chatterjee, T. L. Steck, P. S. Low, G. F. Musso, E. T. Kaiser, P. H. Rogers, and A. Arnone. 1984. The interaction of hemoglobin with the cytoplasmic domain of band 3 of the human erythrocyte membrane. *J. Biol. Chem.* 259:10238–10246.

47. Salhany, J. M. 2008. Kinetics of reaction of nitrite with deoxy hemoglobin after rapid deoxygenation or predeoxygenation by dithionite measured in solution and bound to the cytoplasmic domain of band 3 (SLC4A1). *Biochemistry.* 47:6059–6072.

48. Chu, H., A. Breite, P. Ciraolo, R. S. Franco, and P. S. Low. 2008. Characterization of the deoxyhemoglobin binding site on human erythrocyte band 3: implications for O2 regulation of erythrocyte properties. *Blood.* 111:932–938.

49. Weber, R. E., W. Voelter, A. Fago, H. Echner, E. Campanella, and P. S. Low. 2004. Modulation of red cell glycolysis: interactions between vertebrate hemoglobins and cytoplasmic domains of band 3 red cell membrane proteins. *Am. J. Physiol. Regul. Integr. Comp. Physiol.* 287:R454–R464.

50. Campanella, M. E., H. Chu, and P. S. Low. 2005. Assembly and regulation of a glycolytic enzyme complex on the human erythrocyte membrane. *Proc. Natl. Acad. Sci. USA.* 102:2402–2407.

51. Gladwin, M. T., J. H. Crawford, and R. P. Patel. 2004. The biochemistry of nitric oxide, nitrite, and hemoglobin: role in blood flow regulation. *Free Radic. Biol. Med.* 36:707–717.

52. De Rosa, M. C., C. C. Alinovi, A. Galtieri, A. Russo, and B. Giardina. 2008. Allosteric properties of hemoglobin and the plasma membrane of the erythrocyte: new insights in gas transport and metabolic modulation. *IUBMB Life.* 60:87–93.

53. Shaklai, N., and V. S. Sharma. 1980. Kinetic study of the interaction of oxy- and deoxyhemoglobins with the erythrocyte membrane. *Proc. Natl. Acad. Sci. USA.* 77:7147–7151.

54. Aprelev, A., M. A. Rotter, Z. Etzion, R. M. Bookchin, R. W. Briehl, and F. A. Ferrone. 2005. The effects of erythrocyte membranes on the nucleation of sickle hemoglobin. *Biophys. J.* 88:2815–2822.

55. Hirsch, R. E., A. C. Rybicki, N. A. Fataliev, M. J. Lin, J. M. Friedman, and R. L. Nagel. 1997. A potential determinant of enhanced crystallization of Hbc: spectroscopic and functional evidence of an alteration in the central cavity of oxyHbC. *Br. J. Haematol.* 98:583–588.

56. Elbaum, D., R. E. Hirsch, and R. L. Nagel. 1980. Decreased binding of 2,3-diphosphoglycerate to deoxy hemoglobin S: a polymerization-independent functional abnormality. University of Chicago Symposium on Sickle Cell Disease, Vol. 1, Molecular Basis of Mutant Hemoglobin Dysfunction. P. B. Sigler, editor. Elsevier-North-Holland, New York. 253–258.

57. Hirsch, R. E., L. J. Juszczak, N. A. Fataliev, J. M. Friedman, and R. L. Nagel. 1999. Solution-active structural alterations in liganded hemoglobins C (β6 Glu $\rightarrow$Lys) and S (β6 Glu $\rightarrow$ Val). *J. Biol. Chem.* 274:13777–13782.

58. Chen, Q., C. Bonaventura, R. L. Nagel, and R. E. Hirsch. 2002. Distinct domain responses of R-state human hemoglobins A, C, and S to anions. *Blood Cells Mol. Dis.* 29:119–132.

59. Juszczak, L. J., C. Fablet, V. Baudin-Creuza, S. Lesecq-Le Gall, R. E. Hirsch, R. L. Nagel, J. M. Friedman, and J. Pagnier. 2003. Conformational changes in hemoglobin S (βE6V) imposed by mutation of the beta Glu7-beta Lys132 salt bridge and detected by UV resonance Raman spectroscopy. *J. Biol. Chem.* 278:7257–7263.

60. Brittain, N. J., C. Erexson, L. Faucette, J. Ward, H. Fujioka, T. E. Wellems, and R. M. Fairhurst. 2007. Non-opsonising aggregates of IgG and complement in haemoglobin C erythrocytes. *Br. J. Haematol.* 136:491–500.

61. Brugnara, C., A. S. Kopin, H. F. Bunn, and D. C. Tosteson. 1985. Regulation of cation content and cell volume in hemoglobin erythrocytes from patients with homozygous hemoglobin C disease. *J. Clin. Invest.* 75:1608–1617.

62. Romero, J. R., S. M. Suzuka, R. L. Nagel, and M. E. Fabry. 2004. Expression of HbC and HbS, but not HbA, results in activation of K-Cl cotransport activity in transgenic mouse red cells. *Blood.* 103:2384–2390.

63. Conley, C. L. 1964. Pathophysiological effects of some abnormal hemoglobins. *Medicine (Baltimore).* 43:785–787.

64. Goodman, S. R., A. Kurdia, L. Ammann, D. Kakhniashvili, and O. Daescu. 2007. The human red blood cell proteome and interactome. *Exp. Biol. Med. (Maywood).* 232:1391–1408.

65. Pasini, E. M., M. Kirkegaard, D. Salerno, P. Mortensen, M. Mann, and A. W. Thomas. 2008. Deep-coverage mouse red blood cell proteome: a first comparison with the human red blood cell. *Mol. Cell. Proteomics.* 7:1317–1330.

66. Zabrocki, P., K. Pellens, T. Vanhelmont, T. Vandebroek, G. Griffioen, S. Wera, F. Van Leuven, and J. Winderickx. 2005. Characterization of alpha-synuclein aggregation and synergistic toxicity with protein tau in yeast. *FEBS J.* 272:1386–1400.

67. Galkin, O., and P. G. Vekilov. 2004. Mechanisms of homogeneous nucleation of polymers of sickle cell anemia hemoglobin in deoxy state. *J. Mol. Biol.* 336:43–59.